Journal of Materials and Electronic Devices 1 (2022) 1-6

Structural and morphological characterization of rare earth element doped NiO thin films produced by dynamic sol-gel spin coating method

*[1]Ezgi Gürgenç and [1]Aydın Dikici

[1]Firat University, Technology Faculty, Energy Systems Engineering Department, Elazig, Turkey

In this study, pure nickel oxide (NiO) and cerium (Ce) doped NiO thin films in different ratios (5 mol.% and 10 mol.%) were coated on the microscope glass by dynamic sol-gel spin coating method. Nickel (II) acetate tetrahydrate was used as a nickel (Ni) source and Cerium (III) nitrate hexahydrate was used as a Ce source. The coating process was carried out in 30 seconds at 2000 rpm and two layers of coating were made. The samples were annealed at 450 °C for 1 hour. The structural properties of the samples were determined by X-ray diffraction analysis (XRD). The morphologies of the coating surfaces were characterized by field emission scanning electron microscopy (FE-SEM) and energy dispersion X-ray spectrometry (EDX). Ce-doped NiO thin films were produced successfully. Lattice parameters and unit cell volume increased with increasing Ce doping. Particles with different morphologies were formed with the doping of Ce. With the Ce doping, rougher surfaces were formed and it increased as the doping ratio increased. The results show that the structural and morphological properties of NiO thin films can be changed with Ce doping. It is thought that the produced Ce-doped NiO thin films can find use area in opto-electronic devices.

Keywords: *Cerium, Nanomaterial, NiO, Opto-electronic, Rare earth element, Thin film.*

Submission Date:03 February 2022
Acceptance Date: 01 May 2022

**Corresponding author: ezgigurgenc89@gmail.com*

1. Introduction

The demand for cost-effective opto-electronic devices has increased significantly in recent years. Because of this situation, studies on transparent conductive oxides (TCO) have become very interesting for researchers all over the world. The first thing that comes to mind when talking about ITOs is In_2O_3:Sn (ITO), but the expensiveness of this material has led researchers to less costly alternatives. These alternatives are metal oxides such as doped and undoped ZnO, TiO2, NiO and BaSnO3 [1]. Among these metal oxides, NiO is a p-type transparent semiconductor with a wide and direct band gap in the range of 3.6 – 4.0 eV [2]. In addition, having good thermoelectric and catalytic properties, excellent durability, electrochemical stability, low material cost, being a promising ion storage material in terms of cyclic stability, wide-aperture optical density and the possibility of production with various techniques make NiO very interesting [3, 4]. Due to these interesting properties, NiO can find use in many applications such as sensing devices, catalysts, p-type transparent conductive electrode devices, electrochromic devices, fuel cells, dye-sensitized solar cells and electronic batteries [1]. Increasing the functionality and performance of NiO is of interest to researchers due to its wide range of uses [5]. NiO is generally not stoichiometric, ie the Ni:O ratio deviates from 1. For this reason, adding different additives such as La, Cd, Mg, K, Cu, Eu and Ce to NiO affects its properties and enables it to produce devices with different performances [1, 4, 6]. In recent years, studies have accelerated to obtain better optical

and magnetic properties by adding Rare Earth (RE) 3d ion to NiO. RE atoms have special 4f shells and are excellent alternatives for luminescence centers of doped materials due to the narrow emission line passage of –4f or 4f–5d. The transition plays an important role in the absorption of RE atoms in the UV range. The energy transfer process from the excited semiconductor host to the doped lanthanide atoms supports the doped nanoparticles to bypass the absorption of optical centers with an outstanding improvement in luminescence properties. Of the RE elements, cerium (Ce) has good potential in optical properties and biomedical applications. For this reason, it is an interesting subject to investigate in different applications as an additive material [7].

Doped and undoped NiO thin films are successfully produced by different methods such as chemical vapor deposition, lasering, RF Sputtering, sol–gel and spray pyrolysis. The sol-gel process has some advantages such as being simple, low cost, and allowing thin film deposition in a large area [3, 8, 9].

Studies such as the production of Ce doped nanoparticles, their characterization and use as a gas sensor, their use in supercapacitor applications and investigation of their antibacterial properties are available in the literature [7, 10-13]. Arif et al. produced 1% wt., 2.5% wt. and 5% wt. Ce doped NiO thin films by sol-gel spin coating method. They investigated the structural and optical properties of the thin films they produced [1]. In the literature, it was seen that the studies on the production of Ce doped NiO thin films and the investigation of their structural and morphological properties were limited, and it was decided to carry out this study. Unlike the literature studies, in our opinion, since it has not been studied in the literature before, in the present study, highly Ce doped (5% mol. and 10% mol. 10%) NiO thin films were produced by dynamic sol-gel spin coating method. The structural and morphological properties of the produced thin films were investigated.

In this study, pure NiO, 5 mol.% Ce and 10 mol.% Ce doped NiO thin films were coated on microscope glass by dynamic sol-gel spin coating method. The structural and morphological properties of thin films were characterized by XRD, FE-SEM and EDX analyses. Obtained results are explained in detail.

2. Experimental

In this study, Carlo Erba brand Nickel (II) acetate tetrahydrate ($Ni(OCOCH_3)_2 \cdot 4H_2O$) was used as a Nickel source and Sigma Aldrich brand Cerium (III) nitrate hexahydrate ($Ce(NO_3)_3 \cdot 6H_2O$) was used as a cerium (Ce) source. Microscope glasses were cut in pieces of 10 x 10 mm^2 and ultrasonically cleaned with acetone, ethyl alcohol and deionized water, respectively. Glass pieces were dried with nitrogen gas and stored in a vacuum container until coating process. For the sol-gel required for NiO coatings, 0.5 M ($Ni(OCOCH_3)_2 \cdot 4H_2O$) was added to 10 ml of 2-methoxyethanol and mixed in a magnetic stirrer until all the particles were dissolved. Then 0.5 M monoethanolamine was added to this mixture. This mixture was stirred at 80 °C for 2 hours to obtain a sol-gel. In the Ce doped samples, ($Ce(NO_3)_3 \cdot 6H_2O$) was added to 10 ml of 2-methoxyethanol together with ($Ni(OCOCH_3)_2$ $4H_2O$) a total amount of 0.5 M in the ratios of 5 mol.% and 10 mol.%, and all the processes mentioned above were repeated. All sol-gels obtained were left to rest for 24 hours at room temperature and coated with dynamic sol-gel spin coating method on the optical microscope glass, which was cut and cleaned beforehand. The coating process was carried out in a FYTRONIX brand spin coating device at 2000 rpm in 30 seconds. After the coating process, the samples were dried at 150 °C for 10 minutes and after waiting 10 minutes at room temperature, the second coating layer was coated in the same way. The samples were annealed in the oven at 450 °C for 1 hour. The obtained pure NiO, 5 mol.% Ce, and 10 mol.% Ce doped NiO coated samples were named as NiO, NiO-5Ce and NiO-10Ce, respectively. Structural and morphological properties of thin films were investigated with Zeiss Crossbeam 540 brand FE-SEM device, EDX analysis and PANalytical Empyrean brand XRD device. XRD analyzes of thin films were performed at 45 kV/40 mA, CuKα (λ = 1.5406 ˚A) radiation and 2θ = 20 - 82°.

3. Results and Discussion

The XRD diffraction patterns of the pure and Ce doped NiO thin films are shown in Fig. 1. The crystal planes corresponding to the 2θ angles of the high-density peaks are given in Table 1. XRD diffraction patterns show that the produced thin films are composed of only NiO and all films are in polycrystalline structure. The intense diffraction patterns at 37.31°, 43.26°, 62.86°, 75.53° and 79.38° 2θ values indexed to the cubic Bunsenite phase in the pure NiO sample correspond to the (111), (200), (220), (311), and (222) planes, respectively and match well with JCPDS card number 47–1049 [5]. The diffraction patterns in Ce doped NiO thin films are similar with pure NiO and are in agreement with JCPDS card number 47–1049. As Ce doping ratio increased, the peaks shifted to lower 2θ values and the peak intensities decreased. This is thought to be due to the ionic radius of Ce^{3+} (1.034 Å) higher than that of Ni^{2+} (0.69 Å). The large ionic radius of the doping and host elements can lead to the expansion of the crystal lattice [1, 2, 14]. The high density of the (111) and (200) planes indicates that the pure and Ce doped NiO in different proportions is crystalline. The absence of any secondary phase or impurity in the XRD diffraction patterns proves that pure NiO and Ce doped NiO in different proportions are successfully formed and high purity [2].

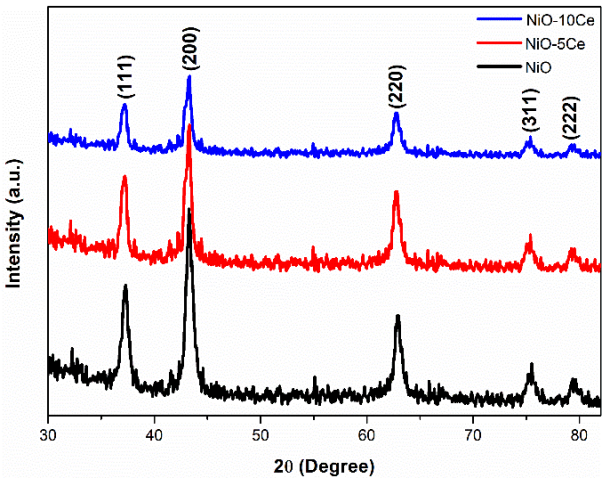

Fig.1. XRD diffraction patterns of the produced thin films.

Table 1. 2θ angles of diffraction planes.

Sample	(111)	(200)	(220)	(311)	(222)
NiO	37.31°	43.26°	62.86°	75.53°	79.38°
NiO-5Ce	37.23°	43.24°	62.86°	75.39°	79.24°
NiO-10Ce	37.17°	43.19°	62.64°	75.32°	79.17°

The interplanar d_{hkl} values of pure NiO and Ce doped NiO thin films were calculated using the Bragg equation [15, 16]. In Table 2, calculated values and the standard values reported in JCPDS card no. 47–1049 are given. The values of produced thin films are compatible with standard values. This shows that undoped and Ce doped NiO thin films at different doping ratios have been successfully produced. The interplanetary distance values of the produced thin films increased with the doping of Ce. This situation is thought to be due to the difference between the ionic radii [6, 15]. The lattice parameters "a" of the NiO cubic structure can be calculated using the following relationship [6, 17];

$$d_{(hkl)} = \frac{a}{\sqrt{(h+k+l)}} \quad (1)$$

Here, h, k, l are miller indices and d is the interplanar distance. The lattice parameters of the thin films were calculated using the (1 1 1) peak for (a = b = c). Unit cell volumes (V) were found using Eq.2 [1, 5].

$$V = a^3 \quad (2)$$

For pure and Ce doped NiO thin films, the average grain sizes (D) can be calculated from the full width of half-maximum (FWHM) of the (111) peak using the Scherrer formula (Eq.3) [18, 19].

$$D = 0.9\,\lambda/\beta\,\cos(\theta) \quad (3)$$

Here, λ is the wavelength of the X-ray in nm, β is the FWHM in radians, and θ is the diffraction angle in degrees.

In Table 3, the structural properties of pure NiO and Ce doped NiO thin films obtained from XRD analysis are given. As can be seen, the lattice parameters and unit cell volumes increased with increasing Ce doping ratio. This may be due to the ionic radius of Ce^{3+} being higher than Ni^{2+}. In case of difference between ionic radii, the host atom can expand the lattice parameters of the main atom [6, 15]. The average grain size of the Ce doped samples is higher than that of pure NiO. XRD results show that pure and Ce doped thin films are successfully coated on microscope glass by dynamic sol-gel coating technique, and XRD analysis results are in agreement with literature studies [1, 5, 6].

Table 2. Interplanar distance values of pure NiO and Ce doped NiO thin films.

hkl	$d_{standart}$ (Å)	NiO d (Å)	NiO-5Ce d (Å)	NiO-10Ce d (Å)
(111)	2.4120	2.4082	2.4132	2.4169
(200)	2.0890	2.0897	2.0907	2.0930
(220)	1.4768	1.4772	1.4772	1.4819
(311)	1.2594	1.2578	1.2598	1.2608
(222)	1.2058	1.2062	1.2079	1.2088

Table 3. Calculated structural properties of the produced thin films with using XRD diffraction patterns.

Numune	hkl	a (Å)	V (Å^3)	D_{111} (nm)
NiO	(111)	4.1711	72.5680	10.4956
NiO-5Ce	(111)	4.1797	73.0201	13.2340
NiO-10Ce	(111)	4.1862	73.3616	13.2050

FE-SEM images and EDX analysis graphics of pure and Ce doped NiO thin films produced by dynamic sol-gel spin coating method are shown in Fig. 2-4. As can be seen, thin films with different morphologies were formed with the doping of Ce. All thin films were composed of nanostructures and the size of these particles increased with increasing Ce ratio. Pure NiO has a homogeneous, void-free and flat coating surface. The coating surface of the NiO sample consists of nano-sized fine grains stacked particles. On the coating surface of the NiO-5Ce sample, on the other hand, nano-sized rod-like structures are seen together with these structures. The surface of this sample is rougher due to the addition of Ce and there are voids in places. The surface of the highly Ce doped sample (NiO-10Ce) is rougher than the others and consisted of stacked nano-structured particles in larger sizes. Similar results were found in studies on Zn and Pb doped thin films, and rougher surfaces were obtained with the doping [5, 19]. According to the EDX analysis results taken from the coating surfaces of the samples, NiO composed of at.% 8.44Ni-91.56O elements, NiO-5Ce composed of at.% 0.79Ni-0.42Ce-98.79O elements and NiO-10Ce composed of at.% 0.47Ni-0.53Ce elements. Ce ratio increased as the additive ratio increased, as expected. The results show that the structural and morphological properties of NiO thin films can be changed with the doping

of Ce and materials with different properties can be produced.

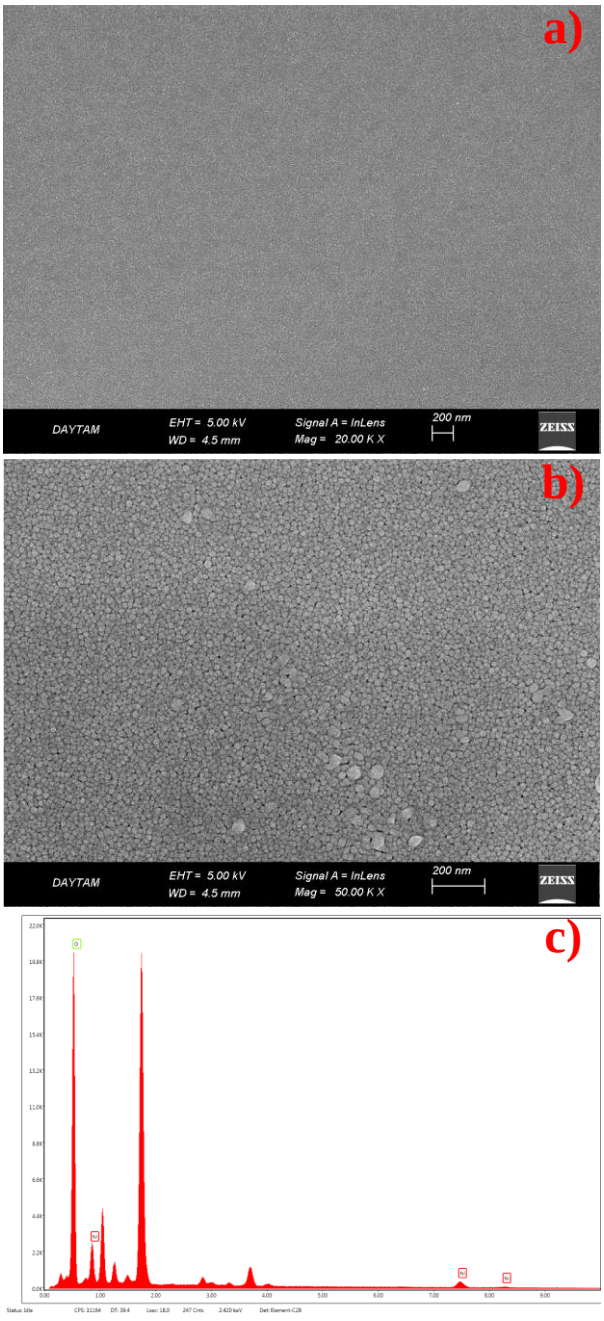

Fig.2. FE-SEM images of the coating surface of the NiO sample a) and b), and c) EDX analysis graph.

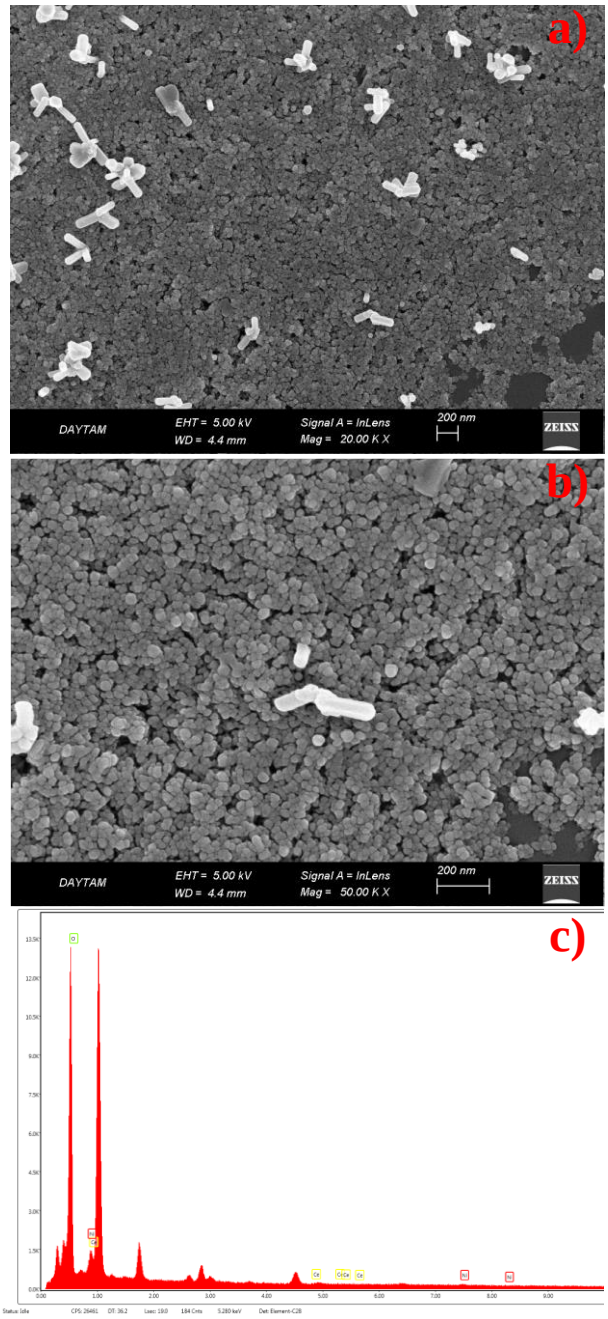

Fig.3. FE-SEM images of the coating surface of the NiO-5Ce sample a) and b), and c) EDX analysis graph.

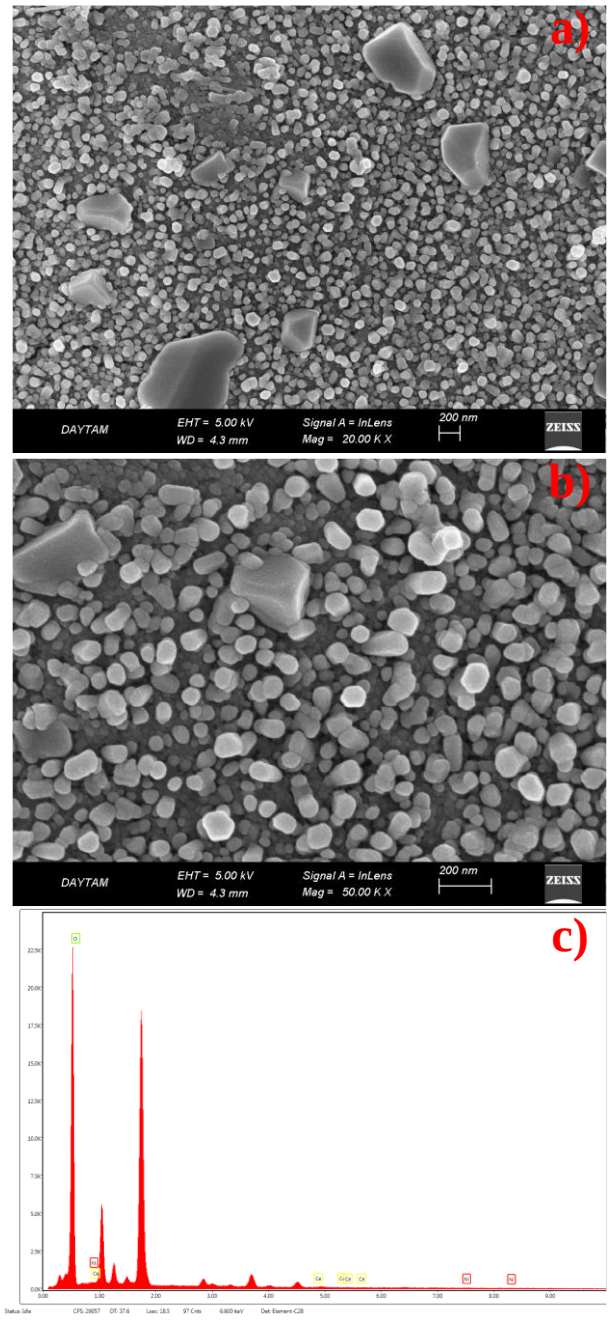

Fig.4. FE-SEM images of the coating surface of the NiO-10Ce sample a) and b), and c) EDX analysis graph.

4. Conclusion

Ce doped NiO thin films were successfully produced by dynamic sol-gel spin coating method. XRD peak intensities decreased with the addition of Ce and characteristic peaks of NiO shifted to lower 2θ values. The structural properties were affected by the addition of Ce, and the lattice parameters increased as the Ce ratio increased. Thin films were composed of stacked nano-sized particles and particle sizes were increased with increasing Ce ratio. As the Ce doping ratio increased, the surfaces became rougher. The results showed that NiO thin films with different properties and parameters can be produced with Ce doping. It is thought that the produced Ce-doped NiO thin films can be used in opto-electronic applications.

Acknowledgment

the author Ezgi GURGENC would like to thank Council of Higher Education (CoHE) for its scholarship support with the 100/2000 Ph.D. scholarship.

References

[1] M. Arif, M. Shkir, V. Ganesh, A. Singh, H. Algarni, S. AlFaify, Superlattices Microstruct. 129 (2019) 230-239.

[2] J.A. Boukhari, A. Khalaf, R.S. Hassan, R. Awad, Appl. Phys. A. 126 (2020) 1-13.

[3] I. Sta, M. Jlassi, M. Hajji, H. Ezzaouia, Thin Solid Films 555 (2014) 131-137.

[4] M. Aftab, M. Butt, D. Ali, F. Bashir, T.M. Khan, Opt. Mater. 119 (2021) 111369.

[5] A.M. El Sayed, Phys. B: Condens. Matter 600 (2021) 412601.

[6] S. Goumri-Said, W. Khan, K. Boubaker, G. Turgut, E. Sönmez, J. Minar, M. Bououdina, M.B. Kanoun, Mater. Res. Bull. 118 (2019) 110525.

[7] M. Abdur Rahman, R. Radhakrishnan, SN Appl. Sci. 1 (2019) 1-9.

[8] M.B. Amor, A. Boukhachem, K. Boubaker, M. Amlouk, Mater. Sci. Semicond. Process. 27 (2014) 994-1006.

[9] K. Zrikem, G. Song, A.A. Aghzzaf, M. Amjoud, D. Mezzane, A. Rougier, Superlattices Microstruct. 127 (2019) 35-42.

[10] R. Gawali, V.L. Patil, V.G. Deonikar, S.S. Patil, D.R. Patil, P.S. Patil, J. Pant, J. Phys. Chem. Solids 114 (2018) 28-35.

[11] P. Saranya, S. Selladurai, New J. Chem. 43 (2019) 7441-7456.

[12] L. Zhu, W. Zeng, J. Yang, Y. Li, Mater. Lett. 251 (2019) 61-64.

[13] S.R. Gawali, D.P. Dubal, V.G. Deonikar, S.S. Patil, S.D. Patil, P. Gomez-Romero, D.R. Patil, J. Pant, ChemistrySelect 1 (2016) 3471-3478.

[14] K. Hussain, N. Amin, M.I. Arshad, Ceram. Int. 47 (2021) 3401-3410.

[15] C. Mrabet, M.B. Amor, A. Boukhachem, M. Amlouk, T. Manoubi, Ceram. Int. 42 (2016) 5963-5978.

[16] A. Patterson, The Scherrer formula for X-ray particle size determination, Phys. Rev. 56 (1939) 978.

[17] R.J.D. Tilley, Crystals and crystal structures, John Wiley & Sons, New York, USA, 2020.

[18] B. Cullity, Elements of X-ray diffraction, addision Wealey pub. company, USA, 1978.

[19] I. Manouchehri, S.A.O. AlShiaa, D. Mehrparparvar, M.I. Hamil, R. Moradian, Optik 127 (2016) 9400-9406.